Passivity-Based Control for Battery Charging/Discharging Applications by Using a Buck-Boost DC-DC Converter

Oscar Danilo Montoya Giraldo
Programa de Ingeniería Eléctrica
y Electrónica, Universidad Tecnológica
de Bolívar, Cartagena, Colombia.
E-mail: omontoya@utb.edu.co
o.d.montoyagiraldo@ieee.org

Alejandro Garcés Ruiz
Programa de Ingeniería Eléctrica
Universidad Tecnológica de Pereira
Pereira, Colombia.
E-mail: alejandro.garces@utp.edu.co

I. Ortega-Velázquez and G. Espinosa-Pérez
Facultad de Ingeniería
Universidad Nacional Autónoma
de México, Coyoacán CDMX, México.
E-mail: isaacortegavel@hotmail.com
gerardoe@unam.mx

***Abstract*—In this paper, a passivity-based control (PBC) theory is applied to control a battery energy storage system (BESS) under current control mode by employing a bidirectional buck-boost DC-DC converter. The proposed controller guarantees globally exponentially stability for the system under closed-loop conditions via proportional control design. An averaging model of the buck-boost DC-DC converter is employed to represent the dynamics of the system via port-Hamiltonian (pH) structure. Simulation results show that a unique control law can be used to the charging or discharging battery process. MATLAB/SIMULINK software is employed to validate the proposed control methodology.**

***Index Terms*—Battery energy storage system (BESS), bidirectional buck-boost DC-DC converter, charge/discharge battery operating modes, current control mode, Lyapunov stability, passivity-based control (PBC).**

I. Introduction

Solid-state electronics has changed the conventional structure of the electrical networks composed mainly by big generation centrals, robust transmission and sub-transmission systems, urban and rural distribution networks and passive loads, for active and smart electrical networks, known as smart grids and microgrids [1]. According to the U.S Department of Energy, "a microgrid is a group of interconnected loads and distributed energy resources with clearly defined electrical boundaries that acts as a single controllable entity with respect to the grid and can connect and disconnect from the grid to enable it to operate in both grid-connected or island modes" [2], [3].

A distributed energy resource interconnected to a microgrid corresponds to dynamical subsystem, which can be controlled inside of the microgrid to help its dynamical performance and improve the global efficiency of the system. The most classical distributed energy resources are composed by renewable energies [4] and energy storage technologies [5].

Chemical energy storage system emerge as one of the most promissory energy storage technology for long term operation, since these technologies can support critical loads for several hours, when the main grid is not available for external events [6], [7] or to supply isolated loads in conjunction with photovoltaic or wind systems [8], among others. The most important chemical technologies for batteries are Lithium-Ion [9], Lead-Acid [10], Nickel-Cadmium or Nickel-Metal-Hydride [11]. The electrical model of each chemical technology as well as their dynamical model can be found in [12], [13].

Different control strategies have been proposed in specialized literature for controlling battery energy storage systems (BESS) integrated with bidirectional buck-boost DC-DC converters, in this sense, a classical PI control approach is highly used due to its simplicity [3], there is also sliding methodologies [14], fuzzy logic controllers [15] and model-predictive controllers [16] and some passive approximations [17].

Unlike the aforementioned works, in this paper explores the interconnection of a (BESS) by using a bidirectional DC-DC buck-boost converter in DC microgrids. The proposed approach considers stability conditions in closed-loop in the sense of Lyapunov via passivity-based control (PBC) theory from the point of view of the dynamics of the error.

The remain of this document is organized as follows: the section II presents the dynamical model of the buck-boost bidirectional DC-DC converter by using a port-Hamiltonian representation. In the section III a passivity-based control approach in presented via Lyapunov analysis by exploiting the bilinear structure of the dynamical model. In the section IV the general control law for the system is obtained, as well as, the desired trajectories of the non-controlled state variables. In the section V the test system parameters and MATLAB/SIMULINK implementation is showed; while in section VI the simulation results are presented with its corresponding analysis in comparison with a classical PI approach. Finally, the section VII presents the main conclusions and suggested future works, followed by the acknowledgments and reference list, respectively.

2166-5478/18/$31.00 ©2018 IEEE
DOI 10.1109/GreenTech.2018.00025

II. Dynamical model

The electrical interconnection of a BESS system by a bidirectional buck-boost DC-DC converter to the equivalent DC grid is depicted in Fig. 1.

The dynamical model of this electrical system can be obtained by applying first and second Kirchhoff's laws for any closed trajectory composed at least one inductor and for any node that contains at least one capacitor. The resulting dynamical model is given below:

$$\begin{aligned} L_1 \tfrac{d}{dt} i_{L1} &= v_b - u v_{C1}, \\ C_1 \tfrac{d}{dt} v_{C1} &= u i_{L1} - i_{L2} - i_D, \\ L_2 \tfrac{d}{dt} i_{L2} &= v_{C1} - R_{dc} i_{L2} - v_{dc}, \end{aligned} \tag{1}$$

where L_1 and L_2 are the battery and grid inductances, C_1 is the capacitance of the buck-boost converter at grid side, u is the average control input, i_D is the current demanded at the point of common coupling, i_{L1} and i_{L2} are the inductance currents, v_{C1} is the voltage in the capacitance, v_b and v_{dc} are the battery and grid voltages, respectively, and R_{dc} emulates the Thevenin equivalent at the point of common coupling.

The dynamical system (1) can be represented as a port-Hamiltonian system as follows:

$$\mathcal{D}\dot{x} - (\mathcal{J}_0 + J_1(u))x + \mathcal{R}x = \zeta, \tag{2}$$

where:

$$\mathcal{D} = \begin{bmatrix} L_1 & 0 & 0 \\ 0 & C_1 & 0 \\ 0 & 0 & L_2 \end{bmatrix}, \quad \mathcal{R} = \begin{bmatrix} 0 & 0 & 0 \\ 0 & 0 & 0 \\ 0 & 0 & R_{dc} \end{bmatrix},$$

$$\mathcal{J}_0 = \begin{bmatrix} 0 & 0 & 0 \\ 0 & 0 & -1 \\ 0 & 1 & 0 \end{bmatrix}, \quad \mathcal{J}_1(u) = \begin{bmatrix} 0 & -u & 0 \\ u & 0 & 0 \\ 0 & 0 & 0 \end{bmatrix},$$

$$x = \begin{pmatrix} i_{L1} & v_{C1} & i_{L2} \end{pmatrix}^T, \quad \zeta = \begin{pmatrix} v_b & -i_D & -v_{dc} \end{pmatrix}^T.$$

The matrix $\mathcal{D}$ is known as inertia matrix, $\mathcal{J}_0 + \mathcal{J}_1(u)$ is the interconnection matrix, R is known as damping matrix, which is positive semidefinite, x is the vector of the state variables and ζ corresponds to the vector of the external inputs.

The dynamical model presented by (2) has the nominal form employed by passivity-based control theory, which makes it the most natural way to control this system, as will be presented in the next section.

Notice that the dynamical model defined by (2) can be used to control the battery current i_{L1} or the voltage at the point of common coupling v_{C1}. In this paper we are interested to control the battery current via passivity-based control technique, which implies that the objective of control can be expressed as:

$$\lim_{t\to\infty} (i_{L1} - i_{L1\star}) = 0, \tag{3}$$

taking into account the following considerations:

- The current $i_{L1\star}$ is known.
- The current i_{L2} and the voltage v_{C1} at the point of common coupling of the buck-boost DC-DC and its local demand i_D are measurable.
- All parameters are defined positive and well-known.

III. Passivity-based control approach

In this section a globally exponentially stable passivity-based controller via proportional gains from the point of view of the dynamics of the error is presented.

Let us consider the dynamical system presented below as function of the error dynamics, this is, $\tilde{x} = x - x_\star$ and $\tilde{u} = u - u_\star$. This dynamical system it is obtained by substituting these definitions on (2),

$$\mathcal{D}\dot{\tilde{x}} = (\mathcal{J}_0 + J_1(u))\tilde{x} - \mathcal{R}\tilde{x} + (J_1(\tilde{u}))x_\star, \tag{4}$$

where the desired dynamics is defined as:

$$\mathcal{D}\dot{x}_\star - (\mathcal{J}_0 + J_1(u_\star))x_\star + \mathcal{R}x_\star = \zeta. \tag{5}$$

Let us define the following Lyapunov candidate function and its temporal derivative.

$$\mathcal{V}(\tilde{x}) = \frac{1}{2}\tilde{x}^T\mathcal{D}\tilde{x} \quad \& \quad \dot{\mathcal{V}}(\tilde{x}) = \tilde{x}^T\mathcal{D}\dot{\tilde{x}}. \tag{6}$$

When it is substituted (4) in (6), we obtain:

$$\dot{\mathcal{V}}(\tilde{x}) = -\tilde{x}^T\mathcal{R}\tilde{x} + \tilde{x}^T\mathcal{J}_1(\tilde{u})x_\star \tag{7}$$

To guarantee that (7) is negative definite, we define the next relation:

$$\mathcal{J}_1(\tilde{u})x_\star = -k_p\tilde{x}, \quad k_p = k_p^T \succ 0. \tag{8}$$

If we define $\mathcal{K} = \mathcal{R} + k_p$, it is easy to prove that for $\beta \leq \lambda_{\min}(\mathcal{D}^{-1}\mathcal{K})$, the dynamical system given by (4) is globally exponentially stable in the sense of Lyapunov.

IV. Controller design

The definition of the general control law depends of the control requirement of the BESS system, in this sense, the objective of control proposed in this paper is to control the current flowing through the battery, this is, i_{L1}. To obtain the control input and the admissible trajectories the set of equations (5) and (8) are solved, which produces:

Control law

The desired control input is obtained from (4) as follows:

$$u_\star = v_{C2\star}^{-1}\left(v_b - L_1\frac{d}{dt}i_{L1\star}\right), \tag{9}$$

where $v_{C2\star}$ is the desired trajectory of the voltage at the common coupling point and $i_{L1\star}$ is the desired reference for the battery current, in other words, it is the objective of control.

The signal control that minimizes tracking error is obtained from (4) as presented below:

$$\tilde{u} = v_{C2\star}^{-1}k_{p1}(i_{L1} - i_{L1\star}), \tag{10}$$

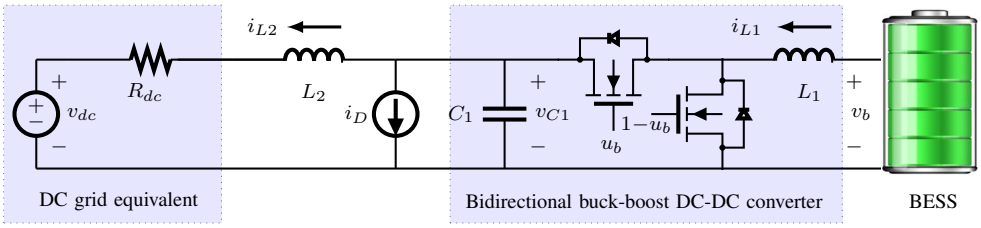

Fig. 1. BESS connection via bidirectional buck-boost DC-DC converter

where k_{p1} is a positive feedback proportional gain.

It is necessary to remember that the control input u is defined by the algebraic sum of (9) and (10).

Admissible trajectories

Admissible trajectories correspond to the trajectories followed by the non-controlled state variables, when the dynamical system is under-actuated, as is the case of the BESS system. In this sense, if the desired trajectory of i_{L1} is defined by $i_{L1\star}$, then, the dynamical behavior of v_{C1} and i_{L2} are given by $v_{C1\star}$ and $i_{L2\star}$. These trajectories are obtained by solving (5).

$$\begin{aligned} C_1 \tfrac{d}{dt} v_{C1\star} &= u_\star i_{L1\star} - i_{L2\star} - i_D, \\ L_2 \tfrac{d}{dt} i_{L2\star} &= v_{C1\star} - R_{dc} i_{L2\star} - v_{dc}. \end{aligned} \tag{11}$$

The differential equations given in (11) correspond to the desired dynamical behaviors of the non-controlled state variables, in this sense, the proposed controller corresponds to a dynamic controller, which is continuously corrected as function of the desired states. For this reason, it is important to point out that the solution of (11) is indispensable to fulfill the control objective. One of the most important situation in this context corresponds to the initial conditions of the desired states, which are carefully selected to avoid singularities in the control law (see (10)). These initial conditions are selected different from zero and limited by the operative characteristics in the electrical components of the network to improve the dynamical performance of the proposed controller.

V. Test system and MATLAB/SIMULINK implementation

The proposed electrical connection for the BESS showed in Fig. 1 is employed as test system. The electrical parameters are given in Table I.

The design and implementation of the test system is made on MATLAB/SIMULINK 2017a by using a desk-computer INTEL(R) Core(TM) $i5-3550$, 3.50 GHz, 8 GB RAM with 64 bits Windows 7 Professional. This implementation and its corresponding controller are presented in Fig. 2.

VI. Simulation results

The numerical validation of the proposed controller is made by two simulating scenarios. The First scenario shows the capacity of the proposed controller to tracking an arbitrary desired trajectory for the battery current; while the second scenario shows the possibility to make load tracking.

A. Parametrization and simulating conditions

All simulation was made bu using MATLAB/SIMULINK 2017a software and SimPowerSystem library by using the circuit diagram presented in 2. As switching frequency, we select 5 kHz. The proportional gain for the PBC approach is $k_p = 1000$, while in case of classical PI control the proportional an integral gains were selected in $k_p = 0.2$ and $k_i = 110$, respectively.

For the implementation of the PI control we use the software available in [18] provided by [3].

B. Battery's current control

The control of the battery current is made by selecting an arbitrary desired current reference $i_{L1\star}$ such that, has positive and negative values as well as ramps and step changes. Additionally, for this simulating scenario, we consider that $i_D = 0$ without loss of generality.

In Fig. 3 the desired current and the battery current are depicted; besides, the tracking error is also shown.

Notice that, in case of references with changes given by ramps the tracking error holds around to zero, this is, the desired and output currents are close as can be seen in Figs. 3a and 3b from $t = 0$ to $t = 1$; however, when the reference current experiments step changes, the output current is limited by the battery characteristics, which implies that its rate of change is limited, producing an appreciable tracking error (see Fig. 3 from $1 \leq t \leq 1.1$). In this sense, we can concluded that the rate of change for any current reference need to be limited by the battery features to avoid unnecessary control efforts.

Comparing the dynamical response given by the conventional PI controller and the proposed PBC approach, it is clear that both controllers make the control task; nevertheless, the

TABLE I
Electrical parameters of the test system

Parameter	Symbol	Value	Unity
Battery inductance	L_1	$40e^{-3}$	H
Grid inductance	L_2	$10e^{-3}$	H
Grid resistance	R_{dc}	1	Ω
Capacitance	C_1	$1200e^{-6}$	F
Battery nominal voltage	v_b	12	V
Battery nominal Current	i_b	10	A
Battery state of charge	SoC	80	%
Grid voltage	v_{dc}	48	V

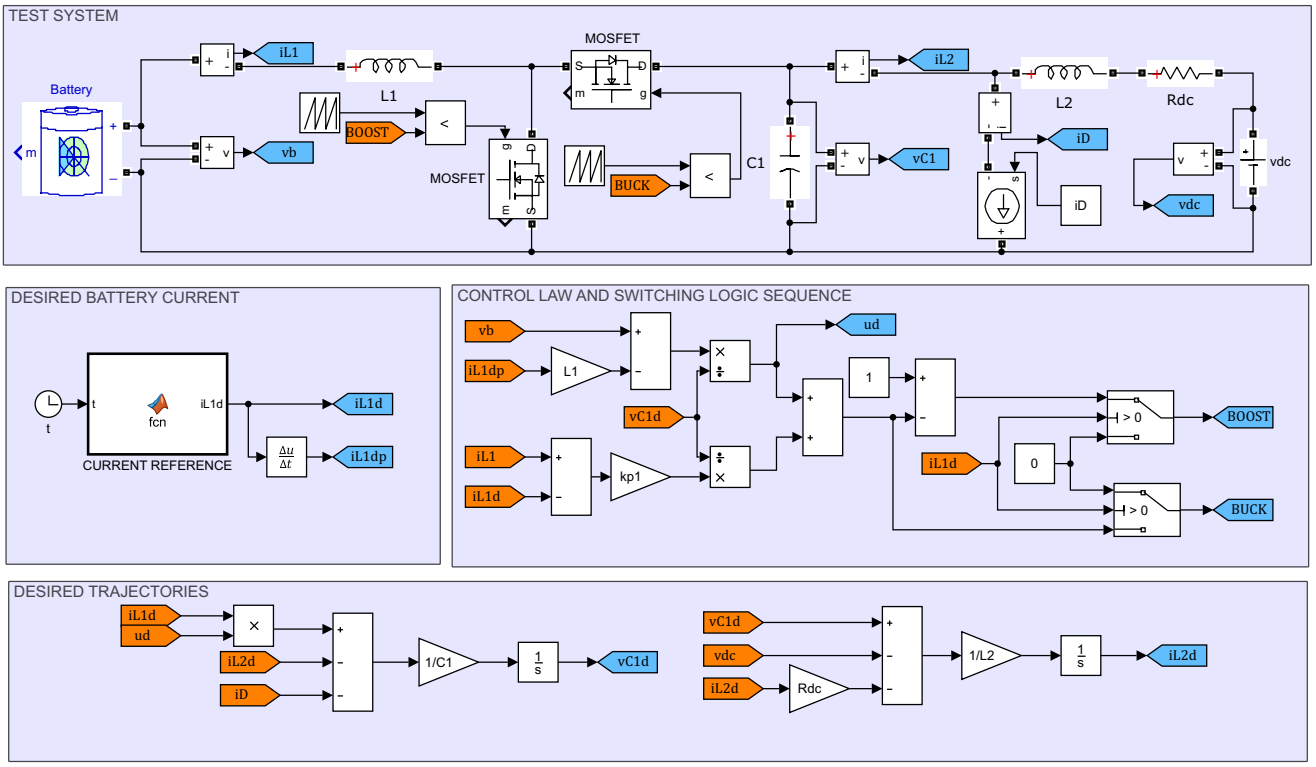

Fig. 2. MATLAB/SIMULINK implementation of the test system and the proposed controller

PBC controller has less tracking error (see Fig. 3c), mainly when the reference curve is a ramp type.

On the other hand, in Fig. 4 the dynamical behavior of voltage in the capacitor and the grid current are presented.

In Fig. 4 it is clear that the dynamical behavior of the voltage in the capacitor is defined by the total current flowing through the inductance and resistance of the grid, which implies that under steady state conditions the this voltage differs from v_{dc} in the voltage droop caused by the resistance, and they are equals only when i_{L2} is zero. In addition, the PI controller produces oscillations with more amplitude, in comparison with the proposed PBC approach.

C. Load tracking

The proposed controller can be used to make load tracking, this is, that the battery supports all current demanded for the load i_D. In this sense, to define the current reference $i_{L1\star}$, the following relation needs to be fulfilled:

$$i_{L1\star} = \frac{v_{C1}}{v_b} i_D. \tag{12}$$

Notice that (12) is the relation of transformation of the buck-boost DC-DC converter.

In Fig. 5 the desired and battery current as well as grid side current are depicted.

Recall that after the initial transitory ($t < 1s$), the desired current depicted in Fig. 5a and battery current showed in Fig. 5 have the same behavior, in other words, the proposed control allows to achieve i_{L1} to $i_{L1\star}$ defined by (12). This implies that the current supplied by the grid holds around zero value as shown in 5c. Additionally, due to the commutation losses in the buck-boost converter (non-modeled in this paper), there exist a small error between the power demanded by the load ($v_{D1} i_D$) and the power generated by the battery ($v_b i_{L1}$). This difference is compensated dynamically by the grid side current i_{L1}, specially when the reference variates as ramp curve, as can be seen during the period of time comprehend from $t = 4s$ to $t = 8s$ in Fig. 5c.

It is important to mention that in the case of load tracking the classical PI control and the proposed PBC approach present a quite similar dynamical behavior, which occurs since the load has soft changes minimizing the transitory effects in the controller performances.

Finally, in Fig. 6 the battery variables are presented for the load tracking case.

In Figs. 6a and 6b are shown the dynamical behaviors of the battery voltage and its corresponding state of charge for classical PI proposed PBC controller approaches. Notice that both dynamical behaviors follow the same trajectory with reduced oscillations fulfilling the control task adequately.

D. General comments

In terms of dynamical performances of the proposed PBC method and classical PI approach they present a quite similar behavior; nevertheless, the passivity-based control method

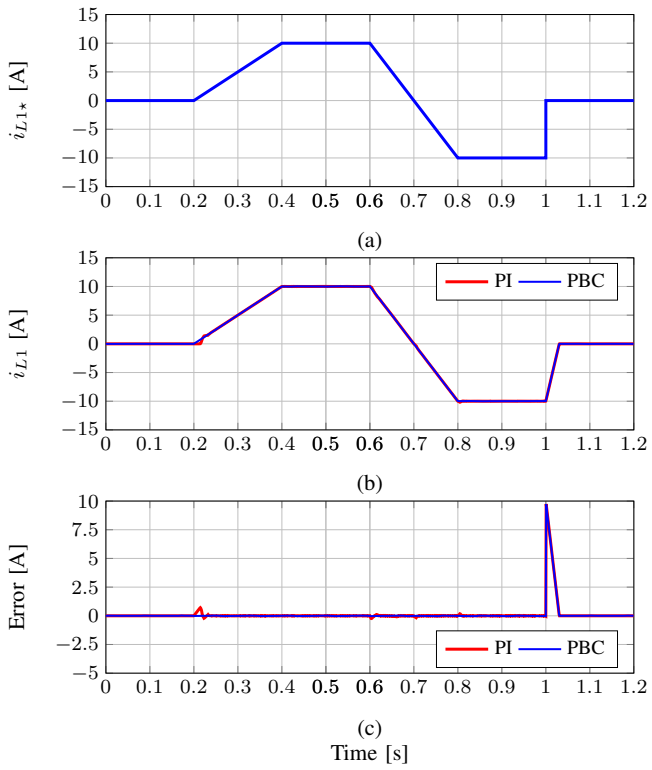

Fig. 3. Desired and battery currents: a) reference value $i_{L1\star}$, b) battery's current i_{L1}, and c) tracking error

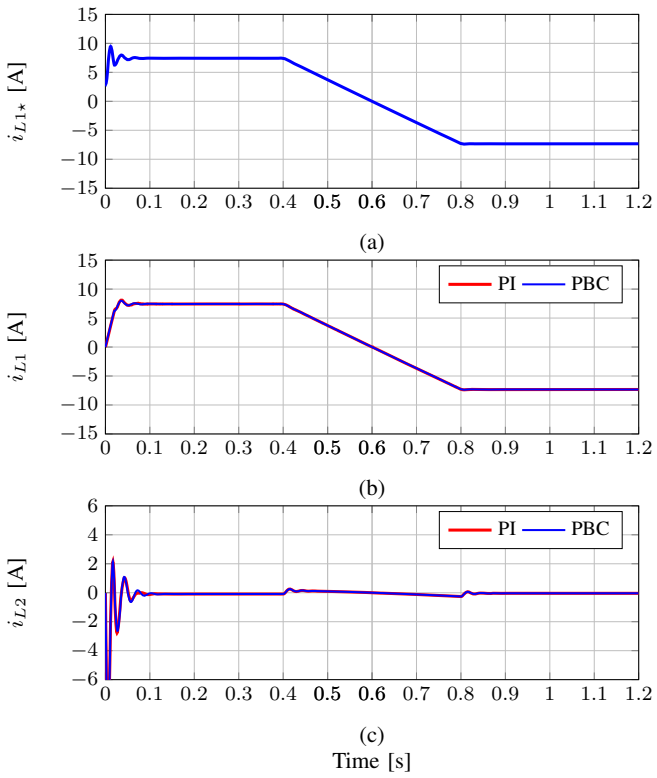

Fig. 5. Dynamical behavior of the system currents: a) battery's desired current, b) battery's current, and c) grid side current

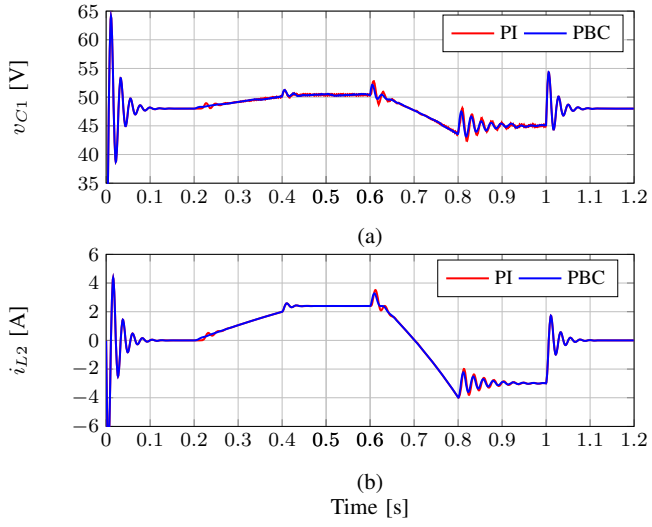

Fig. 4. Grid side state variables: a) v_{C1} and b) i_{L1}

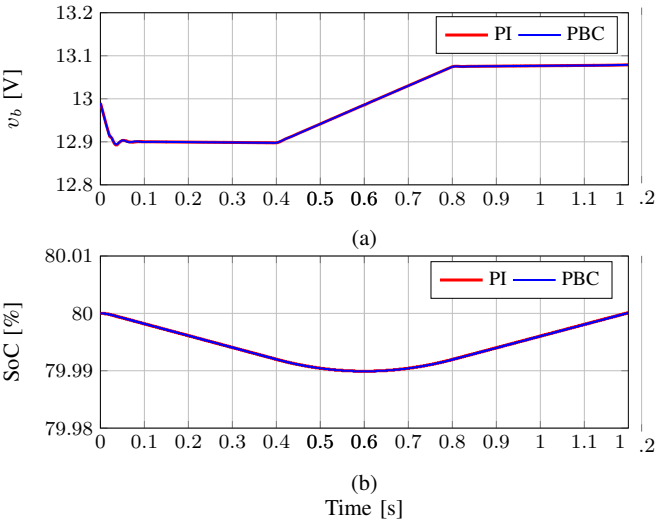

Fig. 6. Grid side state variables: a) v_{C1} and b) i_{L1}

requires only one control gain to achieve the control objective, while the conventional PI control requires two control gains, which difficult its parametrization when in compared to the proposed approach.

The test system analyzed in this paper is only validated via simulation scenarios, for this reason, there are not discussed practical issues about experimental validation; however, for this purposes the general characteristics of BESS and its

integration in DC power grids can be studied in [3].

VII. Conclusions and future works

An exponentially stable controller was designed to operate a BESS system integrated to DC grid with a buck-boost bidirectional converter via passivity-based proportional controller. The proposed controller uses a unique control law to charge or discharge the BESS system with only one control parameter, which simplifies the controller design in comparison to the classical PI approach.

The proposed controller can be used for photovoltaic applications integrated with boost unidirectional converters, due to the dynamical model of the boost converter is identically to the dynamical model presented in this paper for the buck-boost bidirectional converter, which implies that the control input designed can be used to operate a PV array under current control mode.

A modification of proposed PBC approach can be made to control the voltage profile in the grid side of the buck-boost converter, to support dynamical loads in isolated distributed energy resource applications. Additionally, integral actions can be added to the proposed controller to minimize steady state errors preserving asymptotic stability in the sense of Lyapunov via passivity-based PI control theory.

Acknowledgments

This work was supported by the National Scholarship Program Doctorates of the Administrative Department of Science, Technology and Innovation of Colombia (COLCIENCIAS), by calling contest 727-2015 and PhD program in Engineering of the Universidad Tecnolgica de Pereira.

References

[1] R. Strzelecki and G. Benysek, *Power Electronics in Smart Electrical Energy Networks*, Springer-Verlag London, Ed. Springer, 2008. [Online]. Available: http://www.springer.com/la/book/9781848003170

[2] S. Parhizi, H. Lotfi, A. Khodaei, and S. Bahramirad, "State of the art in research on microgrids: A review," *IEEE Access*, vol. 3, pp. 890–925, 2015.

[3] M. Saleh, Y. Esa, Y. Mhandi, W. Brandauer, and A. Mohamed, "Design and implementation of CCNY DC microgrid testbed," in *2016 IEEE Industry Applications Society Annual Meeting*, Oct 2016, pp. 1–7.

[4] J. J. Justo, F. Mwasilu, J. Lee, and J. W. Jung, "AC-microgrids versus DC-microgrids with distributed energy resources: A review," *Renewable Sustainable Energy Rev.*, vol. 24, pp. 387–405, 2013. [Online]. Available: http://dx.doi.org/10.1016/j.rser.2013.03.067

[5] R. Elliman, C. Gould, and M. Al-Tai, "Review of current and future electrical energy storage devices," in *2015 50th International Universities Power Engineering Conference (UPEC)*, Sept 2015, pp. 1–5.

[6] Y. Yang, Q. Ye, L. J. Tung, M. Greenleaf, and H. Li, "Integrated Size and Energy Management Design of Battery Storage to Enhance Grid Integration of Large-Scale PV Power Plants," *IEEE Trans. Ind. Electron.*, vol. 65, no. 1, pp. 394–402, Jan 2018.

[7] I. Hadjipaschalis, A. Poullikkas, and V. Efthimiou, "Overview of current and future energy storage technologies for electric power applications," *Renewable Sustainable Energy Rev.*, vol. 13, no. 6, pp. 1513–1522, 2009.

[8] R. Teodorescu, M. Liserre, and P. Rodriguez, *Grid converters for photovoltaic and wind power systems*. John Wiley & Sons, 2011, vol. 29.

[9] P. G. Bruce, S. A. Freunberger, L. J. Hardwick, and J.-M. Tarascon, "Li-O2 and Li-S batteries with high energy storage," *Nature materials*, vol. 11, no. 1, pp. 19–29, 2012.

[10] J. F. Manwell and J. G. McGowan, "Lead acid battery storage model for hybrid energy systems," *Sol. Energy*, vol. 50, no. 5, pp. 399–405, 1993.

[11] H. Ogawa, M. Ikoma, H. Kawano, and I. Matsumoto, "Metal hydride electrode for high energy density sealed nickel-metal hydride battery," in *Power Sources 12: Research and Development in Non-Mechanical Electrical Power Sources*, 1988, pp. 393–409.

[12] L. Gao, S. Liu, and R. A. Dougal, "Dynamic lithium-ion battery model for system simulation," *IEEE Trans Compon Packag Technol*, vol. 25, no. 3, pp. 495–505, 2002.

[13] Z. M. Salameh, M. A. Casacca, and W. A. Lynch, "A mathematical model for lead-acid batteries," *IEEE Trans. Energy Convers.*, vol. 7, no. 1, pp. 93–98, 1992.

[14] S. Bock, J. Pinheiro, H. Grundling, H. Hey, and H. Pinheiro, "Existence and stability of sliding modes in bi-directional DC-DC converters," in *Power Electronics Specialists Conference, 2001. PESC. 2001 IEEE 32nd Annual*, vol. 3. IEEE, 2001, pp. 1277–1282.

[15] T.-F. Wu, C.-H. Chang, and Y.-H. Chen, "A fuzzy-logic-controlled single-stage converter for PV-powered lighting system applications," *IEEE Trans. Ind. Electron.*, vol. 47, no. 2, pp. 287–296, 2000.

[16] M. Abedi, B.-M. Song, and R.-Y. Kim, "Nonlinear-model predictive control based bidirectional converter for V2G battery charger applications," in *Vehicle Power and Propulsion Conference (VPPC), 2011 IEEE*. IEEE, 2011, pp. 1–6.

[17] M. R. Mojallizadeh and M. A. Badamchizadeh, "Adaptive Passivity-Based Control of a Photovoltaic/Battery Hybrid Power Source via Algebraic Parameter Identification," *IEEE J. Photovoltaics*, vol. 6, no. 2, pp. 532–539, March 2016.

[18] M. Saleh. (2017, July) Voltage Control DC/DC Bidirectional Converter. Simulink - Software. Mathworks - File Exchange. [Online]. Available: https://www.mathworks.com/matlabcentral/fileexchange/63791-voltage-control-dc-dc-bidirectional-converter